University of Nebraska - Lincoln

DigitalCommons@University of Nebraska - Lincoln

2011

Identification of a Second Mimicry Epitope from *Acanthamoeba castellanii* that Induces CNS Autoimmunity by Generating Cross-Reactive T Cells for MBP 89–101 in SJL Mice

Chandirasegaran Massilamany
University of Nebraska-Lincoln, cmassilamany@unl.edu

Oluwatoyin A. Asojo
University of Nebraska Medical Center, oasojo@unmc.edu

Arunakumar Gangaplara
University of Nebraska - Lincoln

David J. Steffen
University of Nebraska-Lincoln, dsteffen1@unl.edu

Jay Reddy
University of Nebraska - Lincoln, jayreddy@unl.edu

Follow this and additional works at: https://digitalcommons.unl.edu/vbsjayreddy

Part of the Biological Phenomena, Cell Phenomena, and Immunity Commons, Medical Biochemistry Commons, Medical Molecular Biology Commons, and the Nervous System Diseases Commons

Identification of a Second Mimicry Epitope from *Acanthamoeba castellanii* that Induces CNS Autoimmunity by Generating Cross-Reactive T Cells for MBP 89–101 in SJL Mice

Chandirasegaran Massilamany[1], Oluwatoyin A. Asojo[2], Arunakumar Gangaplara[1], David Steffen[1], and Jay Reddy[1]

[1]School of Veterinary Medicine and Biomedical Sciences, University of Nebraska-Lincoln, Lincoln, Nebraska, U.S.A.
[2]Department of Pathobiology and Microbiology, College of Medicine, University of Nebraska Medical Center, Omaha, Nebraska, U.S.A.

Correspondence to: J. Reddy, School of Veterinary Medicine and Biomedical Sciences, University of Nebraska-Lincoln, Lincoln, Nebraska, U.S.A.; E-mail: jayreddy@unl.edu

Abstract

We had previously reported that *Acanthamoeba castellanii* (ACA) contains a mimicry epitope for proteolipid protein 139–151 capable of inducing central nervous system (CNS) autoimmunity in SJL/J mice. We now present evidence that ACA also contains a mimicry epitope for myelin basic protein (MBP) 89–101, a derivative from amoebic nicotinamide adenine dinucleotide dehydrogenase subunit 2 (NAD). The epitope, NAD 108–120, contains a discontinuous stretch of six amino acids in the core region (VVFFKNIILIGFL) sharing 46% identity with MBP 89–101 (VHFFKNIVTPRTP; identical residues are underlined). SJL mice immunized with NAD 108–120 develop encephalomyelitis similar to the disease induced by the cognate peptide. We demonstrate that NAD 108–120 induces T cells that cross-react with MBP 89–101; the antigen-sensitized T cells, which produce predominantly T helper (T_h) 1 and T_h17 cytokines, transfer disease in naive SJL recipients reminiscent of the disease induced with MBP 89–101. This is the first report to demonstrate that a solitary microbe can induce CNS autoimmunity by generating cross-reactive T cells for multiple myelin antigens.

Introduction

Multiple sclerosis (MS) is believed to be an autoimmune disease of the central nervous system (CNS), and autoreactive T cells and B cells have been implicated in the disease pathogenesis (1, 2). Three candidate autoantigens—myelin proteolipid protein (PLP), myelin basic protein (MBP) and myelin oligodendrocyte glycoprotein (MOG)—have been identified in MS pathogenesis, and MS patients show varying degrees of T cell and antibody responses to all three (1, 3–5). The importance of these antigens has been well studied in the rodent models of experimental autoimmune encephalomyelitis (EAE) by inducing the disease with the immunodominant epitopes of myelin antigens, the phenotypes of which vary with different genetic backgrounds. For example, MBP $_{Ac}$ 1–11 induces the monophasic form of EAE in B10.PL or PL/J mice (IA^u); MOG 35–55 induces the chronic progressive form in C57BL/6 mice (IA^b) and PLP 139–151 induces relapsing remitting paralysis, whereas MBP 89–101 induces the chronic or relapsing form of EAE in SJL mice (IA^s) (6–11). Likewise, the MBP fragment encompassing 89–101/87–99, restricted by the MHC class II allele RT1D, induces the monophasic form of EAE in Lewis rats (11). These phenotypes resemble some of the clinical features of MS, thus making the observations seen in rodents relevant to humans.

Exposure to environmental microbes such as viruses and bacteria has long been suspected in the initiation of MS, but direct evidence has not been proven clinically. MS epidemics have been shown to be primarily associated with exposure to virus infections, and the roles of human herpes virus (HHV)-6 and Epstein-Barr virus (EBV) are being actively investigated (12–14). It has been suggested that microbial infections can lead to bystander activation (15, 16) or de novo generation of autoreactive cells as a result of the release of cryptic antigenic determinants and/or epitope spreading in infected individuals (17). Alternatively, microbial products bearing the sequences identical to those in self-antigens can lead to the generation of cross-reactive cells, a phenomenon known as molecular or antigenic mimicry (18).

In our efforts to identify the disease-inducing microbial mimics for PLP 139–151, we recently identified a novel epitope from *Acanthamoeba castellanii* (ACA), 83–95, which induces EAE in SJL mice by generating cross-reactive cells for PLP 139–151 (19). We also demonstrated that the pathogenicity of ACA 83–95-induced PLP-specific cells differs by gender but is independent of cytokine responses, in that the cross-reactive cells generated in males fail to induce the disease in females but not vice versa, suggesting modulation of cross-reactive immune responses by sex hormones (20). Regardless of gender, however, the TCR vβ usage of cross-reactive T cells induced with ACA 83–95 differs from that of cells induced with PLP 139–151. By using PLP 139–151/IA^s tetramers, we showed that the TCR vβ2-expressing PLP

139–151-specific CD4 cells are skewed in mice immunized with ACA 83–95, indicating that exposure to microbial mimics can lead to the selective expansion of T cell clones that differ from those generated by cognate epitopes (20). In this report, we present evidence that ACA also contains a mimicry epitope for MBP 89–101 and that the epitope spanning 108–120 amino acids represents the nicotinamide adenine dinucleotide dehydrogenase subunit 2 (NAD) of *Acanthamoeba*. We demonstrate that NAD 108–120 induces clinical and histological features of EAE similar to those induced by the cognate peptide in SJL mice by generating cross-reactive T cells for MBP 89–101 and pro-inflammatory cytokines that favor CNS autoimmunity.

Methods

Mice

Four- to -six-week-old female SJL/J (H-2^s) mice were obtained from the Jackson Laboratory (Bar Harbor, Maine, U.S.A.). The mice were maintained in accordance with the animal protocol guidelines of the University of Nebraska-Lincoln, Lincoln, Nebraska, U.S.A.

Identification of NAD 108–120

Using the LALIGN server (http://www.ch.embnet.org/software/LALIGN_form.html), we searched for identical sequences of MBP 89–101 (VHFFKNIVTPRTP) by comparing ~200 known protein sequences of ACA retrieved from National Center for Biotechnology Information protein database (http://www.ncbi.nlm.nih.gov/). This search resulted in the identification of one epitope spanning the amino acids 108–120 within the NAD of ACA (VVFFKNIILIGFL). All the data were generated using NAD 108–120, except for the homology model for which we used the sequence of NAD 104–118 (NDAAVVFFKNIILIG) by including four additional residues at the N-terminal end and excluding two residues at the C-terminal end from NAD 108–120. The sequence length of NAD 104–118 is consistent with that of MBP 85–99 used in the structural study (21).

Derivation of NAD 104–118/HLA-DR2 homology model

To determine differences between MBP 85–99 and NAD 104–118 with respect to their MHC-contact residues within the binding pockets of HLA-DR2 molecule, we used the crystal structure of HLA-DR2 (DRA, DRB1*1501) complexed with human MBP 85–98 or MBP 86–99 as a reference model (21). The coordinates of these structures (1BX2) were obtained from the Research Collaboratory for Structural Bioinformatics Protein Data Bank (http://www.rcsb.org) and used with the kind permission from Dr. Kai Wucherpfennig, Harvard University, Boston, Massachusetts, U.S.A. The MBP 85–99 reference model was generated by averaging the monomers from the original crystal structure complexed with MBP 85–98 for one monomer and with MBP 86–99 for the other. The averaged structure was three dimensional-protonated and energy-minimized using MMFF94x restraints within MOE software to yield an optimized MBP 85–99/HLA-DR2 structure (Chemical Computing group, Montreal, Canada). The optimized MBP 85–99/HLADR2 model was then used as a template to generate a homology model for HLA-DR2 molecule complexed with NAD 104–118, and the structure was optimized using MOE as described above. The figures of the model were generated using PyMOL software (http://www.pymol.org).

Peptide synthesis and immunization procedures

NAD 108–120, MBP 89–101 and Theiler's murine encephalomyelitis virus (TMEV) 70–86 (WTTSQEAFSHIRIPLP) were synthesized on 9-fluorenylmethyloxycarbonyl chemistry (Neopeptide, Cambridge, Massachusetts, U.S.A.). All peptides were HPLC-purified (>90%) and confirmed by mass spectroscopy and then dissolved in sterile 1× PBS (MBP 89–101) or 1× PBS/dimethyl sulfoxide (DMSO) (NAD 108–120). For disease induction, peptides dissolved in 1× PBS were emulsified in complete Freund's adjuvant (CFA) supplemented with *Mycobacterium tuberculosis* (MTB) H37RA extract (Difco Laboratories, Detroit, Michigan, U.S.A.) to a final concentration of 5 mg ml1, and the peptide emulsions were administered twice in the sternal and inguinal regions with an interval of 7 days (6). In addition, pertussis toxin (PT; List Biological Laboratories, Campbell, California, U.S.A.) was administered (400 ng per mouse) intraperitoneally on day 0 and day 2 post-immunization after the first immunization (6, 8, 22) only. To measure recall responses, MBP 89–101 and NAD 108–120 dissolved respectively, in 1× PBS and DMSO were emulsified in CFA containing no additional MTB extract and administered as above.

Clinical scoring and histopathology

After EAE induction, the mice were monitored for clinical signs of disease and scored as described previously (8, 22): 0, healthy; 1, decreased tail and body tone; 2, a clumsy but otherwise normal gait; 3, definite weakness of one or more limbs; 4, a paraplegic or monoplegic state and 5, a premorbid state. Animals were euthanized during recovery or upon termination on day 30 post-immunization. Brain and spinal cords were collected in 10% phosphate-buffered formalin and analyzed for histological evidence of inflammatory changes (19, 23). After fixation, two brain sections were made; one included cerebrum and hippocampus, and the second included cerebellum and brainstem. In the spinal cord, three sections were made from each segment (cervical, thoracic, lumbar and sacral). All the tissues were stained by hematoxylin and eosin staining. Tissues were blinded to treatment, lesion type was characterized and severity was scored. Severity scores were obtained by counting inflammatory foci in both meninges and parenchyma for all sites. Inflammation was primarily classified as lymphocytic, suppurative or mixed (19, 20). For statistical analysis, counts were added across all sections of brain and spinal cord for each mouse.

Adoptive transfer EAE

Groups of five mice were immunized twice with MBP 89–101 or NAD 108–120 (200 μg per mouse) with a 7-day interval between immunizations; 7 days after the second immunization, the animals were killed, and LNC were prepared from the draining lymph nodes (LNs). LNC were stimulated with Concanavalin-A (Con-A) at a concentration of 1 μg ml^{-1} for 2 days as described previously (6, 24). Viable lymphoblasts were harvested by Ficoll-Hypaque density-gradient centrifugation, and 60 × 10^6 cells were administered intraperitoneally into groups of five naive SJL mice. Additionally, each animal received PT (400 ng) on days 0 and 2 post-transfer, and the animals were monitored for clinical signs of EAE and scored

as above (8, 22, 6). The experiments were terminated on day 21 postinoculation, and the CNS tissues were harvested for histology (19, 20).

Proliferation assay

Groups of mice were immunized with MBP 89–101 or NAD 108–120, and after 10 days, the animals were killed and the draining LN collected to prepare single-cell suspensions. LNC were stimulated with MBP 89–101, NAD 108–120 and TMEV 70–86 (0–100 lgml1) at a cell density of 5×10^6 cells/ml for 2 days in RPMI medium supplemented with 10% fetal bovine serum, 1 mM sodium pyruvate, 4 mM L-glutamine, 1× each of nonessential amino acids and vitamin mixture and 100 U/ml penicillin–streptomycin (Lonza, Walkersville, Maryland, U.S.A.). Cultures were then pulsed with 1 µCi of tritiated ^{3}[H]thymidine per well; 16 h later, the proliferative responses were measured as counts per minute (c.p.m.) using a Wallac liquid scintillation counter (Perkin Elmer, Waltham, Massachusetts, U.S.A.) hereafter called growth medium. We further verified these responses by second-round of re-stimulation with each peptide. LNC obtained from immunized mice were first stimulated with MBP 89–101 or NAD 108–120 (20 µg ml^{-1}) for 2 days and the cells were maintained in growth medium containing IL-2. Viable cells were harvested on day 4 post-stimulation; rested for ~10 to 14 days and the proliferative responses were measured after re-stimulating the cells with the indicated peptides as above.

Intracellular cytokine staining

Mice were immunized with MBP 89-101 or NAD 108–120 and 10 days later, the animals were killed and LN were harvested to prepare LNC. Cells were stimulated with the corresponding peptides for 2 days (20 µg ml^{-1}) and the cultures were maintained in IL-2 medium. Viable lymphoblasts were harvested on day 4 and stimulated for 4.5 h with phorbol 12-myristate 13-acetate (PMA) (20 ng ml^{-1}) and ionomycin (300 ng ml^{-1}) (Sigma–Aldrich, St Louis, Missouri, U.S.A.) in the presence of 2 mM monensin (GolgiStop; BD Pharmingen, San Diego, California, U.S.A.). After staining with anti-CD4 and 7-aminoactinomycin D (7-AAD; Invitrogen, Eugene, Oregon, U.S.A.), cells were fixed, permeabilized and stained with cytokine antibodies or isotype controls (eBioscience, San Diego, California, U.S.A.; 19, 20). Cells were acquired by flow cytometry (FC, FACS Scan; BD Pharmingen), and the frequencies of cytokine-secreting cells were analyzed in the live (7-AAD) CD4+ subset using Flow Jo software (Tree star, Ashland, Oregon, U.S.A.; 19). The clones of cytokine antibodies used were: IL-2 (JES6-5H4), IL-4 (11B11), IL-10 (JES5-16E3), IFN-γ (XMG1.2), IL-17A (eBio 17B7), IL-17F (eBio 18F10), granulocyte macrophage-colony stimulating factor (GM-CSF) (MP122E9) (all from eBioscience) and IL-22 (140301) (R&D Systems, Minneapolis, Minnesota, U.S.A.).

Cytokine ELISA

Supernatants harvested from the above cultures on day 2 were analyzed for cytokines by ELISA (19). The clones of the capture and detection antibody pairs used were: IL-2 (JES6-1A12/JES6-5H4), IL-4 (11B11/BVD6-24G2), IL-10 (JES5-16E3/JES5-2A5), IL-17A (eBio17CK15A5/eBio17B7), IFN-γ (AN-18/R4-6A2), IL-22 (1H8-PWSR/IL-22-JOP) and GM-CSF (MP1-22E9/MP1-31G6) (eBioscience).

Analysis of TCR vβ usage

LNC harvested from the mice immunized with MBP 89–101 or NAD 108–120 were stimulated with the corresponding peptides for 2 days (20 µg ml^{-1}), and the cultures were maintained in IL-2 medium. Cells were harvested on day 4 post-stimulation with peptides and stained with a panel of anti-mouse TCR vβ antibodies: vβ 2, 3, 4, 5.1, 5.2, 6, 7, 8.1, 8.2, 8.3, 9, 10b, 11, 12, 13, 14 and 17a (BD Pharmingen), anti-CD4 and 7-AAD. After acquiring the cells by FC, percentages of TCR vβ$^+$ cells were enumerated in the live (7-AAD$^-$) CD4 population (20).

Statistics

Comparisons of histological disease between groups for inflammatory lesions in the brain and spinal cords were analyzed by two-sided Wilcoxon rank sum test (Mann–Whitney *U*-test). Differences in the cumulative neurological scores of animals with EAE and cytokine secretion with respect to T helper (T$_h$)1, T$_h$2 and T$_h$17 subsets between groups were compared by student's t-test. P < 0.05 values were considered significant.

Results

NAD 108–120 has the structural characteristics of binding to HLA-DR2 molecules

By sequence comparisons, we identified NAD 108–120 as the mimicry epitope for MBP 89–101 showing a similarity of 46.2% and containing a discontinuous stretch of six amino acids (VVFFKNI) in the core region [Figure 1A(i)]. This region within human MBP 85–99 represents an epitope center for recognition by both TCR and auto-antibodies (5). Further more, by crystal study of HLA-DR2 (DRA*0101, DRB1*1501) complexed with human MBP 85–99, the critical MHC-contact residues in MBP 85–99 have been well characterized (21). These include Val89 and Phe92 as primary anchor residues, the latter being the most critical and they bind to P1 and P4 pockets, respectively, in the HLA-DR2 molecule. Three other amino acids, Asn94, Ile95 and Thr97, were identified as the secondary MHC-contact residues binding to the P6, P7 and P9 pockets, respectively (21). Both MBP 85–99 and NAD 104–118 have identical residues in all the above positions, except that Thr97 in MBP 85–99 is substituted with Leu116 in NAD 104–118 [Figure 1A(ii)]. To understand the structural characteristics of MHC binding, we derived a homology model for NAD 104–118/HLA-DR2, which agreed well with the reference structure (Figure 1B), with an overall root mean square deviation of 0.70 Å for all atoms (Figure 1C). Expectedly, the side chains of the conserved Phe 92/111 in MBP 85–99/NAD 104–118 superposed well, and the distance between their alpha carbon atoms was 1.3 Å (Figure 1D). Likewise, while the orientation of Asn (94/113) in MBP 85–99/NAD 104–118 was comparable (1.4 Å), the side chains of Val (89/108) and Ile (95/114) were shifted, and their C-alpha positions were 3.2 and 1.5 Å, respectively (Figure 1D). The position shifts were consistent with energy minimization, and all the identical residues retained their ability to bind in appropriate pockets. The homology model also provided additional information on TCR-contact residues. Previously, it was shown that Phe91 and Lys93 in MBP 85–99 are the major TCR-contact residues, whereas His90 is less criti-
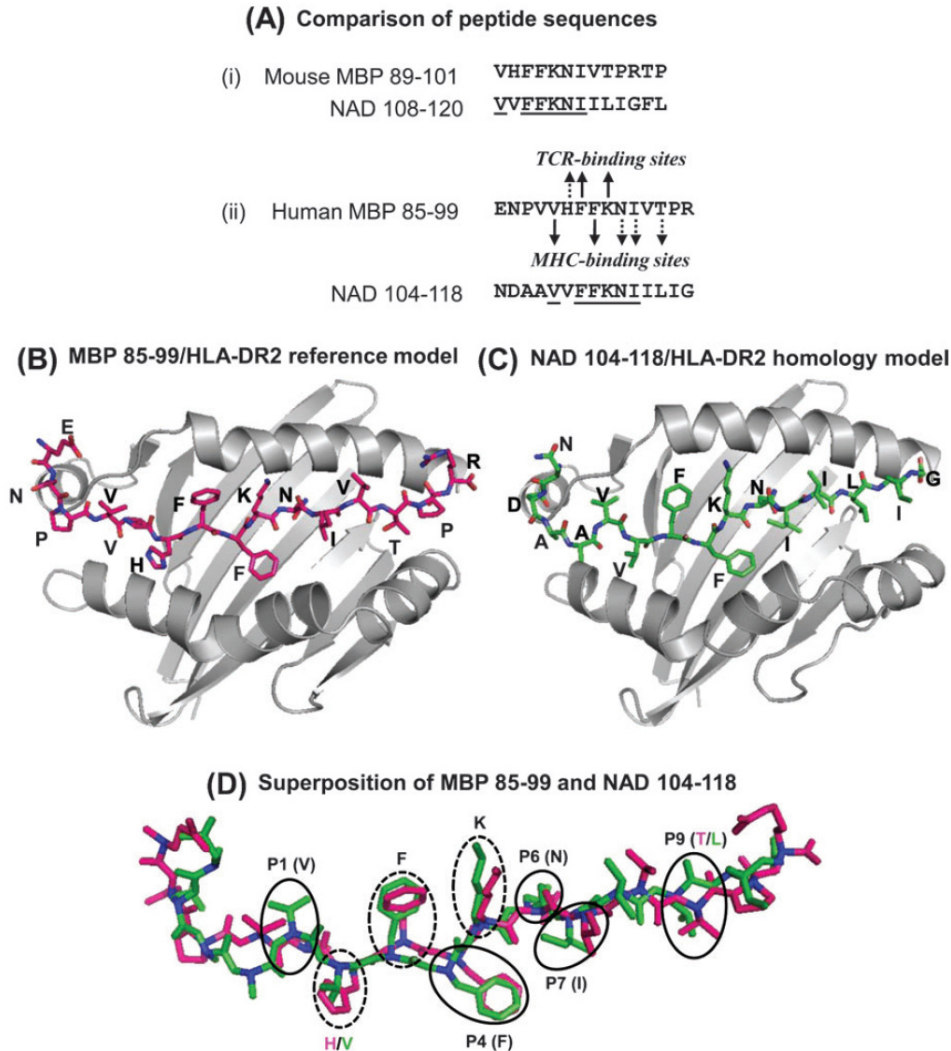
Figure 1. Derivation of homology model for NAD 104–118/HLA-DR2 complex. (A) Comparison of peptide sequences. Amino acid sequences were compared with respect to NAD 108–120 versus mouse MBP 89–101 (i) and NAD 104–118 versus human MBP 85–99 (ii). Identical sequences are underlined. Top arrows, TCR-contact residues; bottom arrows, MHC-anchor residues. Solid arrows, major contacts; dotted arrows, minor contacts. (B) MBP 85–99/HLA-DR2 reference model. The MBP 85–99/HLA-DR2 (DRA, DRB1*1501) reference model was generated by averaging the monomers from the original crystal structure complexed with MBP 85–98 or MBP 86–99 as described in the Methods, and the figure was generated in PyMOL software. (C) NAD 104–118/HLA-DR2 homology model. Using MBP 85–99/HLA-DR2 reference model as a template, homology model for NAD 104–118 complexed with HLA-DR2 was generated as above. (D) Superposition of MBP 85–99 and NAD 104–118. The NAD 104–118/HLA-DR2 complex was superposed over MBP 85–99/HLA-DR2 reference model and the figure was generated in PyMOL software. Solid circles, MHC-binding residues correspond to the indicated pockets (P1, P4, P6, P7 and P9) within HLA-DR2 molecule; dotted circles, TCR-binding residues.

cal for TCR binding (5). The structure of the MBP 85–99/HLA-DR2 complex also revealed that these residues were exposed, allowing them to be easily accessible to TCR (21). Similar to MBP 85–99, NAD 104–118 also has the two major TCR-contact residues, Phe110 and Lys112, whereas His90 is substituted with Val109 [Figure 1A (ii)]. Among these two common residues, the homology model shows that the side chains of Phe91/110 superpose almost identically, whereas Lys (93/112) is more flexible (Figure 1D). Taken together, the homology model suggests that the most critical residue, Phe at positions 111 and 110 in NAD 104–118, is expected to interact with the P4 pocket of the HLA-DR2 molecule and TCR, respectively.

NAD 108–120 induces EAE similar to MBP 89–101

To determine the disease-inducing ability of NAD 108–120, we used active immunization and adoptive transfer EAE protocols. We immunized groups of mice and followed the disease course for 30 days. The CNS tissues were collected for histology during remission or upon termination of experiments. We noted that NAD 108–120 induced the disease dose dependently ,in that a dose of 50 µg per mouse did not induce the disease, whereas the disease severity was moderate in animals that received 100 µg (Figure 2A). In contrast, a dose of 200 µg NAD 108–120 resulted in EAE severity comparable to that induced by MBP 89–101, with a similar mean day of onset (12.00 ± 1.32 versus 12.10 ± 0.94) and mean maximum

score (1.90 ± 0.23 versus 2.00 ± 0.15) [Table 1(i)], including the cumulative scores (16.00 ± 2.54 versus 18.00 ± 2.87) [Figure 2C(i)]. Consistent with clinical EAE, mice that received NAD 108–120 showed dose-dependent perivascular infiltrations in the brains and spinal cords, and the inflammatory foci in animals that received 200 µg of NAD 108–120 were comparable to those immunized with MBP 89–101 [Table 1(i)]. Likewise, regardless of the immunogens used, inflammatory changes were found in both meninges and parenchyma, with a tendency for lesions to be seen more in meninges than parenchyma as evaluated at different time points (day 16 or 30) post-immunization, and the infiltrations were composed predominantly of lymphocytes, with few histiocytes and plasma cells [Figure 3A]. Verification of these results in naive mice did not reveal any of the changes described above (data not shown). We next verified encephalitogenic potential of NAD 108–120 in adoptive transfer experiments by injecting the lymphoblasts obtained from mice immunized with the corresponding peptides as described previously (24, 25). As shown in Figure 2B, LNC from mice immunized with MBP 89–101 or NAD 108–120 induced the disease in all the naive SJL recipients (100%) with comparable mean days of onset (11.40 ± 0.51 versus 11.80 ± 0.73) and mean maximum scores (2.20 ± 0.20 versus 2.00 ± 0) [Table 1(ii)]. The disease severity,
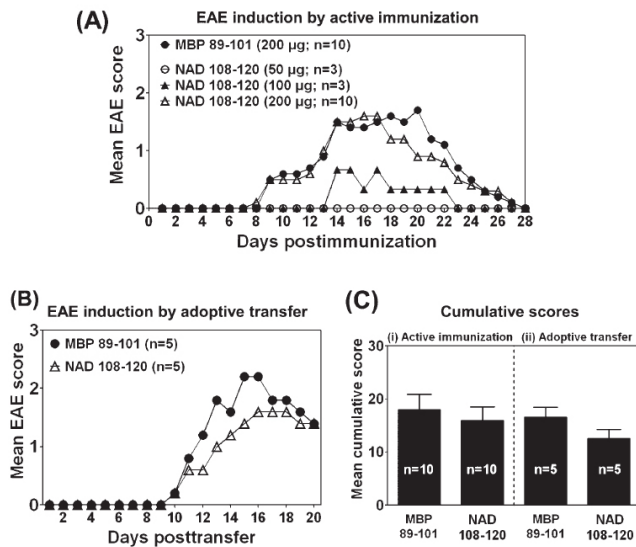

Figure 2. NAD 108–120 induces autoimmune encephalomyelitis similar to MBP 89–101. (A) EAE induction by active immunization. Groups of SJL mice were immunized with the indicated amounts of MBP 89–101 or NAD 108–120 in CFA twice with an interval of 1 week and PT was administered on day 0 and 2 after the first immunization. The mice were monitored for clinical signs of EAE and scored. (B) EAE induction by adoptive transfer. Seven days after the second immunization with MBP 89–101 or NAD 108–120, the mice were killed and LNC were harvested from the draining LN. LNC were stimulated with Con-A for 2 days and viable lymphoblasts were injected into naive SJL mice intraperitoneally. Each mouse received PT (400 ng) on day 0 and 2 post-transfer and the animals were observed for signs of EAE and scored. Mean values for a group of mice are shown. (C) Cumulative scores. Cumulative scores were obtained by adding the neurological scores for each mouse and compared between groups. Each bar represents mean ± SEM values for a group of mice.

however, tended to be lower in mice that received cells from NAD 108–120 than those that received MBP 89–101 sensitized cells as evaluated based on cumulative scores (12.60 ± 1.69 versus 16.60 ± 1.81) [Figure 2C(ii)] and the inflammatory foci in CNS tissues [Table 1(ii); Figure 3B]. Taken together, the data suggest that NAD 108–120 is an encephalitogenic mimicry epitope of MBP 89–101 and disease induction requires the mediation of antigen-sensitized T cells.

MBP 89–101 and NAD 108–120 induce cross-reactive T-cell responses

Induction of EAE with MBP 89–101 in SJL mice is typically mediated by CD4 cells (8, 22, 26). The fact that CNS inflammation induced by NAD 108–120 was similar to that induced by MBP 89–101 suggests that the mimicry epitope can induce the generation of cross-reactive T cells for MBP 89–101. To examine this possibility, we stimulated LNC from mice immunized with NAD 108–120 or MBP 89–101 with the corresponding peptides dissolved in 1× PBS, and their recall responses were measured based on ^{3}[H]thymidine incorporation. Expectedly, both MBP 89–101 and NAD 108–120 induced the dose-dependent proliferative responses to the respective peptides, but a fraction of these cells also responded to unimmunizing peptides (Figure 4). For example, LNC from MBP 89–101 immunized mice responded to MBP peptide, and approximately one-third of the MBP-reactive T cells also showed response to NAD 108–120 [Figure 4A (i)]. Similar patterns were observed when NAD 108–120 sensitized LNC were examined for their reactivity to NAD and MBP peptides although the reactivity for the latter was relatively low [Figure 4A(ii)]. The responses were antigen specific since LNC from mice immunized with either MBP 89–101 or NAD 108–120 did not respond to the control peptide (TMEV 70–86). We verified these data by second-round of restimulation with MBP 89–101 or NAD 108–120. Expectedly, LNC cultures prepared from MBP 89–101 immunized mice responded dose dependently to both MBP 89–101 (7.9-fold) and NAD 108–120 [4.9-fold; Figure 4B(i)]. Similar patterns were noted when the cultures obtained from NAD 108–120 immunized mice were re-stimulated with NAD 108–120 (2.9-fold) and MBP 89–101 [2.8-fold; Figure 4B(ii)]. The data demonstrate that MBP 89–101 and NAD 108–120 induce antigen-specific cross-reactive T-cell responses.

LNC sensitized with MBP 89–101 or NAD 108–120 produce cytokines that favor CNS autoimmunity

The hallmark of encephalitogenic T cells is their ability to secrete T_h1 and T_h17 cytokines; in addition, mice deficient in GM-CSF show resistance to the development of EAE (27–29). We examined Th1 (IL-2 and IFN-γ), T_h2 (IL-4 and IL-10), T_h17 (IL-17A, IL-17F and IL-22) cytokines and GM-CSF in LNC obtained from mice immunized with MBP 89–101 or NAD 108–120 by both intracellular cytokine detection and cytokine ELISA. Figure 5(A) shows that the cells capable of secreting all the cytokines tested except IL-4 were present in the cultures stimulated with MBP 89–101 or NAD 108–120. Their proportions were dominated by both T_h1 (12.25 ± 2.14 versus 11.18 ± 2.65) and Th17 (9.05 ± 1.32 versus 6.13 ± 1.23) cytokine-secreting cells (Figure 5A and B). Within the T_h17 subset, however, frequencies of IL-22secreting cells were higher than IL-17F and IL-17A or combination of the two

Table 1. Clinical and histologic EAE in SJL mice induced with MBP 89–101 and NAD 108–120[a]

Treatment	Clinical disease			No. of inflammatory foci		
	Incidence (%)	Mean day of onset[b]	Mean maximum score[b]	Meninges	Parenchyma	Total
(i) EAE induction by active immunization						
MBP 89–101						
200 µg	9/11 (81.8)	12.10 ± 0.94	2 ± 0.15	4.18 ± 1.36	2.27 ± 0.75	6.45 ± 2.01
NAD 108–120						
50 µg	2/4 (50)	0	0	1 ± 0.71	0 ± 0	1 ± 0.71
100 µg	3/4 (75)	14 ± 0.00	1 ± 0.00	6.5 ± 4.57	0.75 ± 0.48	7.25 ± 4.99
200 µg	11/11 (100)	12 ± 1.32	1.09 ± 0.23	9.09 ± 3.80	3.73 ± 1.14	12.82 ± 4.53
(ii) EAE induction by adoptive transfer						
MBP 89–101	5/5(100)	11.4 ± 0.51	2.2 ± 0.2	10.4 ± 6.65	11 ± 7.07	21.4 ± 13.69
NAD 108–120	5/5(100)	11.8 ± 0.73	2 ± 0	6 ± 2.51	1.4 ± 0.93	7.4 ± 2.04

Scoring scale: 0, healthy; 1, decreased tail and body tone; 2, a clumsy but otherwise normal gait; 3, definite weakness of one or more limbs; 4, a paraplegic or monoplegic state; 5, a premorbid state.
[a]Numbers are mean ± SEM.
[b]Represents only mice that showed clinical disease.

(Figure 5A). Nonetheless, comparison of MBP-versus NAD-stimulated cultures for frequencies of cells producing different cytokines did not reveal any striking differences except that T_h17 cytokine-secreting cells tended to be low in NAD 108–120 cultures. Verification of these results by cytokine ELISA revealed no detectable amounts of IL-4, but T_h1 and T_h17 cytokines were detected with no skewing toward IL-22 secretion (Figure 5C). Comparative analysis revealed that MBP 89–101 stimulated culture supernatants had more of both T_h1 and T_h17 cytokines, including GM-CSF, than those from NAD 108–120 sensitized cultures; the respective amounts were 701.36 ± 169.19 versus 72.50 ± 30.94; 451.51 ± 77.99 versus 45.23 20.73 and 128.58 ± 48.59 versus 8.00 ± 2.25 pg ($P \leq 0.001$). Taken together, the data suggest that NAD 108–120 can induce the generation of T_h1 and T_h17 cytokine-secreting cells but to a lesser magnitude than MBP 89–101.

T cells sensitized with MBP 89–101 or NAD 108–120 use similar TCR vβs

To determine whether T cells sensitized with cognate and mimicry epitopes use similar TCR vβs, we analyzed their usage in CD4 T cells in cultures prepared from mice immunized with the corresponding peptides by FC. We noted that expression of TCRvβs were found consistently in the order of vb4, vb2, vb17a, vβ6, vβ14, vβ3, vβ7, vβ5.1 and vβ5.2 in the cultures stimulated with either MBP 89–101 or NAD 108–120 (Figure 6). While, the vβ usage was mostly constituted by vβ4, vβ2, vβ17a, vβ6 and vβ14, there were no significant differences between the cultures stimulated with MBP 89–101 or NAD 108–120 (59.45 versus 57.56%), suggesting that cognate and mimicry epitopes sensitize similar T-cell repertoires.

Discussion

In this report, we present evidence that NAD 108–120 induces autoimmune encephalomyelitis through the generation of cross-reactive T cells for MBP 89–101. MBP is one of the major candidate autoantigens identified in EAE/MS pathogenesis (2, 30). The mouse MBP sequence spanning amino acids 89–101 has been shown to induce EAE in SJL mice (8, 31, 32), and the human MBP 85–99 sequence equivalent to mouse MBP 89–101 matches 100%. Numerous studies indicate that T cells and B cells from MS patients show reactivity to MBP; in addition, MBP 85–99 has been recognized as one of the major immunodominant epitopes in MS patients bearing HLA-DR2 haplotype (HLA-DRB*1501, DQB1*0602) (5, 33, 34). Indeed,

the core motif of the 10-amino acid fragment within MBP 85–99 (VVHFFKNIVT) represents an epitope center for recognition by both MHC/TCR and auto-antibodies; for the latter, however, the FFK sequence has to be conserved (5). Similar to MBP 85–99, NAD 108–120 also possesses all the major MHC- and TCR-contact residues but the question is whether it can elicit cross-reactive T cells and trigger CNS autoimmunity in humans. To address this possibility, we derived a homology model for NAD 104–118/HLA-DR2 to determine whether the configuration and orientations of the critical MHC-and TCR-contact residues in cognate and mimicry epitopes follow similar patterns. The homology model indicated that orientation of the side chains of the two critical MHC-anchor residues Ph92/111 and Asn94/113 and one major TCR-contact residue, Phe91/110 in MBP 85–99/NAD 104–118 superposed comparably suggesting that the mimicry epitope can potentially anchor HLA-DR2 molecule similar to MBP 85–99 and also to be recognized by MBP 85–99 specific TCR. We also propose that NAD 108–120 has the potential to activate MBP-specific B cells. We make this prediction because the stretch of three amino acids, FFK within the epitope center of MBP 85–99 (VVHFFKNIVT) is highly critical for MBP-specific auto-antibody recognition (5). Ironically, microbial peptides bearing sequences identical to the epitope center of MBP 85–99 have been previously shown to bind MBP-specific auto-antibodies derived from MS brain tissue and the binding correlated with the number of identical residues in the epitope center (5). These include one peptide from L2 protein of human papillomavirus (VHFFK-I), which bound best to MBP-specific antibody followed by the peptides derived from *Bacillus subtilis* (FFKNI) and *Clostridium cellulare* (FFKN). The fact that NAD 108–120 also possesses identical residues similar to the above (V-FFKNI) suggests that NAD 108–120 can also bind to MBP-specific auto-antibodies.

In this study, using both active and AT-EAE protocols, we show that NAD 108–120 induces autoimmune encephalomyelitis in SJL mice by generating cross-reactive T cells for MBP 89–101 and the T cells preferentially produce T_h1 and T_h17 cytokines that favor CNS autoimmunity. The induction of cross-reactive T cell responses was expected because the core region of NAD 108–120 has a high degree of similarity with MBP 89–101. This region potentially contains critical MHC–TCR-contact residues as shown in human MBP 85–99 (21), which might have led to the generation of cross-reactive T cells for MBP. However, the inflammatory foci in the CNS
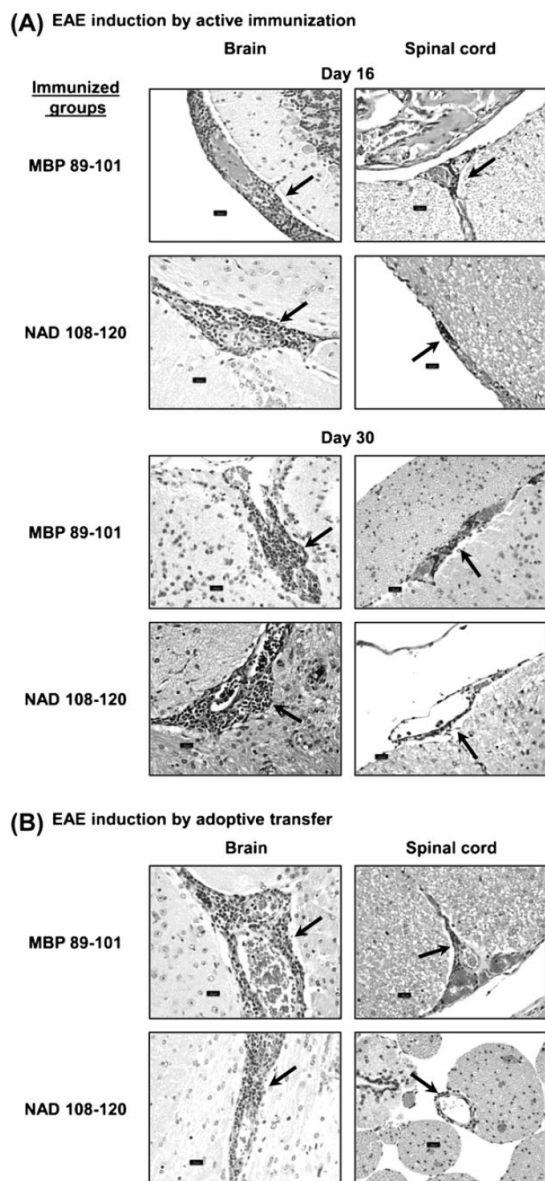
Figure 3. Histological evaluation of CNS inflammation induced with MBP 89–101 or NAD 108–120. (A) EAE induction by active immunization. Brains and spinal cords harvested on day 16 and day 30 from mice immunized with MBP 89–101 or NAD 108–120 show perivascular lymphocytic infiltrations (arrows) as evaluated by hematoxylin and eosin staining. (B) EAE induction by adoptive transfer. Hematoxylin and eosin sections show mixed perivascular cuffing (arrows) in the brains and spinal cords of mice that received lymphocytes generated from mice immunized with MBP 89–101 or NAD 108–120. Original magnification, 3400 (bar = 20 μm).

lesions induced by these cells tended to be low [Table 1(ii)], which may be due to the presence of a low proportion of T_h17 cytokine-secreting cells (Figure 5). Both T_h1 and Th17 cells are critical to the mediation of CNS autoimmunity (27, 28), but the proportion of cytokines produced by each subset appears to be antigen dependent. For example, in our hands, we noted that antigen-specific cells from SJL mice immunized with PLP 139–151 secrete a higher proportion of both IFN-γ and IL-17, with a tendency for IFN-γ to be higher than IL-17, as
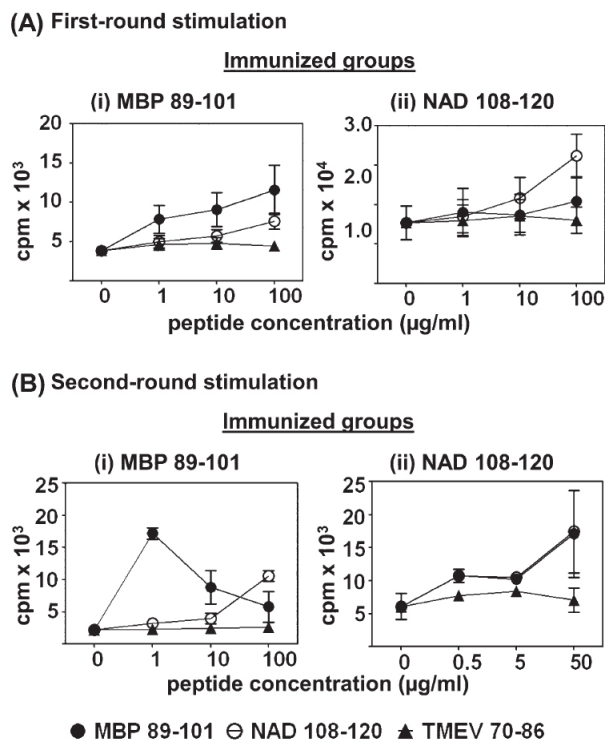

Figure 4. MBP 89–101 and NAD 108–120 induce cross-reactive T-cell responses. (A) First-round stimulation. Groups of mice were immunized with MBP 89–101 or NAD 108–120 and 10 days later, animals were killed and the draining LN were collected. LNC were stimulated with the indicated peptides for 2 days followed by pulsing with ^{3}[H]thymidine, the incorporation of which was measured as c.p.m. 16 h later. TMEV 70–86, control. Mean ± SEM values for a group of mice are shown each involving up to five mice per group (MBP 89–101, n =7; NAD 108–120, n = 4). (B) Second-round stimulation. LNC obtained from MBP 89–101 or NAD 108–120 immunized mice were stimulated with the respective peptides twice with an interval of approximately 10–14 days as described in the Methods and the proliferative responses were measured as above. Mean ± SEM values for a group of mice each involving two to three mice are shown (MBP 89–101, n =3; NAD 108–120, n =4).

evaluated using IA^s/PLP 139–151 tetramers (20). Although cytokines induced with MBP 89–101 or NAD 108–120 follow the same pattern as above, the IL-22-secreting cells dominated Th17 responses. While IL-17 and IL-22 participate in innate immune responses (35, 36), IL-22 can exert both pro- and anti-inflammatory effects, but the role of IL-22 in organ-specific autoimmune diseases is controversial. For example, IL-22 potentiates chronic inflammatory diseases such as arthritis, inflammatory bowel disease and psoriasis but not CNS inflammation in the mouse model of EAE (37–41). Endothelial cells in the blood-brain barrier, however, express receptors for IL-17 and IL-22, and both cytokines can promote CD4 T-cell recruitment in MS lesions (42). On the contrary, IL-22 mediates protection in T-cell-mediated hepatitis and autoimmune myocarditis (40, 43, 44). The finding that IL-22 is a T-cell-derived cytokine, the receptors for which are abundantly expressed in the non-lymphoid tissues, suggests that IL-22 can modulate inflammatory responses in the local milieu (36). Alternatively, multiple cytokines might cooperatively regulate CNS inflammation.
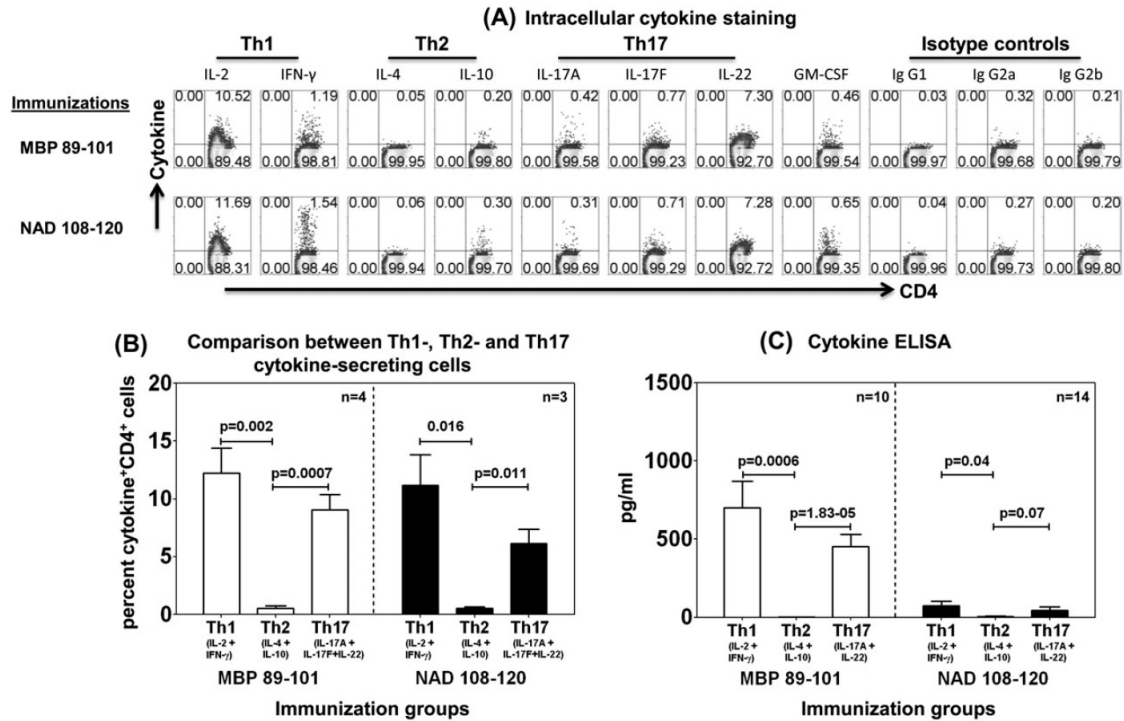
Figure 5. MBP 89–101 and NAD 108–120 induce similar cytokine profiles. (A) Intracellular cytokine staining. LNC obtained from mice immunized with MBP 89–101 and NAD 108–120 were stimulated with the corresponding peptides for 2 days and the cultures were maintained in IL-2 medium for additional 2 days. Viable lymphoblasts were harvested and stimulated for ;4.5 h with PMA and Ionomycin in the presence of GolgiStop and the cells were stained with anti-CD4 and 7-AAD. After fixation and permeabilization, the cells were incubated with cytokine antibodies and the frequencies of cytokine-secreting cells were determined by FC in the live (7-AAD) CD4 subset. (B) Comparison between T_h1, T_h2 and T_h17 cytokine-secreting cells. Frequencies of CD4 cells producing IFN-γ, IL-4 and IL-10 and IL-17A, IL-17F and IL-22 corresponding to the indicated T_h subsets were added together and compared between groups. (C) Cytokine ELISA. Supernatants harvested on day 2 poststimulation prior to the addition of IL-2 medium from the above cultures were analyzed for cytokines by ELISA. Each bar in the above represents mean ± SEM values for a group of mice.
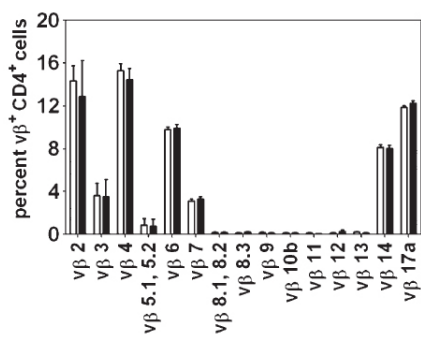

Figure 6. MBP 89–101 and NAD 108–120 sensitized T cells show similar TCR vβ usage. Ten days after immunization with MBP 89–101 or NAD 108–120, the mice were killed and the draining LN were collected. LNC were stimulated with the corresponding peptides for 2 days and maintained in IL-2 medium. Cells were harvested on day 4 post-stimulation and stained with a panel of anti-TCR vβ and anti-CD4 and 7-AAD. After acquiring the cells by FC, percentages of TCR vβ+CD4+ cells were determined in the live (7-AAD) population. Each bar represents mean ± SEM values obtained from three to four experiments each involving one to two mice per group.

We recently reported that the TCR vβ usage of cross-reactive cells for PLP 139–151 induced with ACA 83–95 differs from those induced with PLP 139–151, suggesting a possibility that cognate and mimicry epitopes sensitize distinct T-cell clones (20). One possibility could be that skewed expansion of T-cell clones expressing particular TCR vbs influences the disease outcome, depending on the clones' disease-inducing abilities. Alternatively, exposure to mimicry epitopes might lead to the expansion of hidden clones not usually responsive to cognate peptides. To address these possibilities, we evaluated TCR vβ usage of CD4 cells sensitized with MBP 89–101 or NAD 108–120, but we did not observe any striking differences between the two. Nonetheless, T cells expressing TCR vβ4, vβ2, vβ17a, vβ6, vβ14 and vβ3 were dominant in the cultures stimulated with either peptide, and these profiles were similar to those observed in PLP 139–151-sensitized cells (20, 45, 46). The data suggest that autoreactive T-cell responses generated in a given mouse strain tend to follow a similar pattern of TCR vβ usage regardless of the immunogens used.

MS is a complex disease and no known etiological agents have been identified. Two major factors have been implicated in the initiation of the disease: genetic susceptibility and exposure to environmental factors (2). In support of the latter, exacerbations of MS attacks or temporal alterations in the disease course have been linked to exposure primarily to virus infections such as EBV and HHV-6, but the clinical evidence remains elusive (12–14). The current dogma is that MS does not appear to follow Koch's postulates in that

no single organism appears to trigger MS; rather, exposure to multiple organisms might be critical for MS predisposition (2). We recently reported that ACA contains a mimicry epitope, ACA 83–95, for PLP 139–151, which induces a typical relapsing and remitting type of paralysis in SJL mice by generating PLP-specific T cells (19). In this report, we present evidence that ACA also contains a mimicry epitope, NAD 108–120, but this peptide induces EAE through the generation of T cells that cross-react with yet another myelin antigen, MBP 89–101. While ACA 83–95 is a derivative of rhodanese-related sulfur transferase of *Acanthamoeba*, NAD 108–120 represents NAD, which has been recognized as one of the virulent factors of ACA (47, 48). Presently, it is not known whether these amoebic proteins are processed and present ACA 83–95 and NAD 108–120 in animals infected with *Acanthamoeba*. Proving that mice infected with *Acanthamoeba* show ACA 83–95 or NAD 108–120/NAD 104–118 reactive T cells implies that the amoebic peptides are processed and presented naturally by the APCs. There is an indication that mice infected with ACA show the generation of myelin-and ACA-reactive T cells (Massilamany C., et al, unpublished results). However, it has been shown that the brains of mice infected with *Acanthamoeba culbertsoni* show increased expression of amoebic NAD mRNA (47), and the abundant availability of this amoebic protein can potentially generate cross-reactive immune responses for MBP locally. ACA is a natural CNS pathogen of humans, and while most individuals are exposed to *Acanthamoeba* as indicated by the presence of amoeba-reactive antibodies, they can remain asymptomatic, but the amoebae can induce granulomatous encephalitis in immunocompromised individuals. Whether such exposures can lead to CNS autoimmunity in genetically susceptible individuals remains to be tested. Based on our homology model, we predict that MS patients showing T cell and antibody reactivity to MBP could also react to mimicry epitope by cross reactivity. Experiments are underway to analyze cerebrospinal fluid samples obtained from MS patients to determine the presence of *Acanthamoeba*-specific genomic material or antibodies.

In conclusion, we show that ACA, in addition to possessing a mimicry epitope for PLP 139–151 (19), also contains NAD 108–120 as the mimicry epitope for MBP 89–101. The fact that ACA contains two mimicry epitopes for two different myelin antigens suggests that ACA infection can potentially lead to the generation of multiple myelin-reactive T cells. MS is a multifactorial disease characterized by a plethora of symptoms in the affected individuals, and the proposal that exposure to multiple microbes is a requirement for MS predisposition is gaining importance (2). It is tempting to speculate whether microbes similar to *Acanthamoeba* bearing the mimicry sequences for multiple myelin antigens are likely to be the candidates of disease initiation. To our knowledge, this is the first report to demonstrate that a solitary microbe contains mimicry sequences for more than one autoantigen in the target organs of their natural predilection in the infected individuals. *Acanthamoeba*e are free-living organisms and are ubiquitous in the environment, leading to constant exposure. It is possible that such a co-existence can help microbes acquire some of the genetic elements of their hosts as an evasive mechanism for survival. Alternatively, exposure to such organisms could lead to a break in self-tolerance as a result of antigenic mimicry in genetically susceptible individuals who potentially carry pathogenic autoreactive T-cell and B-cell repertoires.

References

1 Kerlero de Rosbo, N., Milo, R., Lees, M. B., Burger, D., Bernard, C. C. and Ben-Nun, A. 1993. Reactivity to myelin antigens in multiple sclerosis. Peripheral blood lymphocytes respond predominantly to myelin oligodendrocyte glycoprotein. *J. Clin. Invest.* 92: 2,602.

2 Sospedra, M. and Martin, R. 2005. Immunology of multiple sclerosis. *Annu. Rev. Immunol.* 23: 683.

3 Noseworthy, J. H., Lucchinetti, C., Rodriguez, M. and Weinshenker, B. G. 2000. Multiple sclerosis. *N. Engl. J. Med.* 343: 938.

4 Pender, M. P., Csurhes, P. A., Greer, J. M. et al. 2000. Surges of increased T cell reactivity to an encephalitogenic region of myelin proteolipid protein occur more often in patients with multiple sclerosis than in healthy subjects. *J. Immunol.* 165: 5,322.

5 Wucherpfennig, K. W., Catz, I., Hausmann, S., Strominger, J. L., Steinman, L. and Warren, K. G. 1997. Recognition of the immunodominant myelin basic protein peptide by autoantibodies and HLA-DR2-restricted T cell clones from multiple sclerosis patients. Identity of key contact residues in the B-cell and T-cell epitopes. *J. Clin. Invest.* 100: 1,114.

6 Miller, S. D. and Karpus, W. J. 2007. Experimental autoimmune encephalomyelitis in the mouse. *In*: Coligan, J. E., ed., *Current Protocols in Immunology*, Volume 4, p. 15.1.1–15.1.18. Wiley, Hoboken, N.J.

7 Mendel, I., Kerlero de Rosbo, N. and Ben-Nun, A. 1995. A myelin oligodendrocyte glycoprotein peptide induces typical chronic experimental autoimmune encephalomyelitis in H-2b mice: fine specificity and T cell receptor V beta expression of encephalitogenic T cells. *Eur. J. Immunol.* 25: 1,951.

8 Sakai, K., Zamvil, S. S., Mitchell, D. J., Lim, M., Rothbard, J. B. and Steinman, L. 1988. Characterization of a major encephalitogenic T cell epitope in SJL/J mice with synthetic oligopeptides of myelin basic protein. *J. Neuroimmunol.* 19: 21.

9 Tuohy, V. K., Lu, Z., Sobel, R. A., Laursen, R. A. and Lees, M. B. 1989. Identification of an encephalitogenic determinant of myelin proteolipid protein for SJL mice. *J. Immunol.* 142: 1,523.

10 Zamvil, S. S., Mitchell, D. J., Moore, A. C., Kitamura, K., Steinman, L. and Rothbard, J. B. 1986. T-cell epitope of the autoantigen myelin basic protein that induces encephalomyelitis. *Nature* 324: 258.

11 Fritz, R. B. and McFarlin, D. E. 1989. Encephalitogenic epitopes of myelin basic protein. *Chem. Immunol.* 46: 101.

12 Cirone, M., Cuomo, L., Zompetta, C. et al. 2002. Human herpesvirus 6 and multiple sclerosis: a study of T cell cross-reactivity to viral and myelin basic protein antigens. *J. Med. Virol.* 68: 268.

13 Pohl, D. 2009. Epstein-Barr virus and multiple sclerosis. *J. Neurol. Sci.* 286:62.

14 Salvetti, M., Giovannoni, G. and Aloisi, F. 2009. Epstein-Barr virus and multiple sclerosis. *Curr. Opin. Neurol.* 22: 201.

15 Brocke, S., Gaur, A., Piercy, C. et al. 1993. Induction of relapsing paralysis in experimental autoimmune encephalomyelitis by bacterial superantigen. *Nature* 365: 642.

16 Fujinami, R. S., von Herrath, M. G., Christen, U. and Whitton, J. L. 2006. Molecular mimicry, bystander activation, or viral persistence: infections and autoimmune disease. *Clin. Microbiol. Rev.* 19: 80.

17 Miller, S. D., Vanderlugt, C. L., Begolka, W. S. et al. 1997. Persistent infection with Theiler's virus leads to CNS autoimmunity via epitope spreading. *Nat. Med.* 3: 1,133.

18 Fujinami, R. S. and Oldstone, M. B. 1985. Amino acid homology between the encephalitogenic site of myelin basic protein and virus: mechanism for autoimmunity. *Science* 230: 1,043.

19 Massilamany, C., Steffen, D. and Reddy, J. 2010. An epitope from *Acanthamoeba castellanii* that cross-react with proteolipid protein 139-151-reactive Tcells induces autoimmune encephalomyelitis in SJL mice. *J. Neuroimmunol.* 219: 17.

20 Massilamany, C., Thulasingam, S., Steffen, D. and Reddy, J. 2011. Gender differences in CNS autoimmunity induced by mimicry epitope for PLP 139-151 in SJL mice. *J. Neuroimmunol.* 230: 95.

21 Smith, K. J., Pyrdol, J., Gauthier, L., Wiley, D. C. and Wucherpfennig, K. W. 1998. Crystal structure of HLA-DR2 (DRA*0101, DRB1*1501) complexed with a peptide from human myelin basic protein. *J. Exp. Med.* 188: 1,511.

22 Sakai, K., Sinha, A. A., Mitchell, D. J. et al. 1988. Involvement of distinct murine T-cell receptors in the autoimmune encephalitogenic response to nested epitopes of myelin basic protein. *Proc. Natl Acad. Sci. USA* 85: 8,608.

23 Sobel, R. A., Tuohy, V. K., Lu, Z. J., Laursen, R. A. and Lees, M. B. 1990. Acute experimental allergic encephalomyelitis in SJL/J mice induced by a synthetic peptide of myelin proteolipid protein. *J. Neuropathol. Exp. Neurol.* 49:468.

24 Zhao, M. L., Xia, J. Q., and Fritz, R. B. 1992. Experimental allergic encephalomyelitis in susceptible and resistant strains of mice after adoptive transfer of T cells activated by antibodies to the T cell receptor complex. *J. Neuroimmunol.* 40: 31.

25 Panitch, H. S. 1980. Adoptive transfer of experimental allergic encephalomyelitis with activated spleen cells: comparison of in vitro activation by concanavalin a and myelin basic protein. *Cell Immunol.* 56: 163.

26 Pettinelli, C. B. and McFarlin, D. E. 1981. Adoptive transfer of experimental allergic encephalomyelitis in SJL/J mice after in vitro activation of lymph node cells by myelin basic protein: requirement for Lyt 1+ 2-T lymphocytes. *J. Immunol.* 127: 1,420.

27 Bettelli, E., Oukka, M. and Kuchroo, V. K. 2007. T(H)-17 cells in the circle of immunity and autoimmunity. *Nat. Immunol.* 8: 345.

28 Stromnes, I. M., Cerretti, L. M., Liggitt, D., Harris, R. A. and Goverman, J. M. 2008. Differential regulation of central nervous system autoimmunity by T(H)1 and T(H)17 cells. *Nat. Med.* 14: 337.

29 McQualter, J. L., Darwiche, R., Ewing, C. et al. 2001. Granulocyte macrophage colony-stimulating factor: a new putative therapeutic target in multiple sclerosis. *J. Exp. Med.* 194: 873.

30 Lutton, J. D., Winston, R. and Rodman, T. C. 2004. Multiple sclerosis: etiological mechanisms and future directions. *Exp. Biol. Med.* (Maywood) 229: 12.

31 Chou, C. H., Shapira, R. and Fritz, R. B. 1983. Encephalitogenic activity of the small form of mouse myelin basic protein in the SJL/ J mouse. *J. Immunol.* 130: 2,183.

32 Mokhtarian, F., McFarlin, D. E. and Raine, C. S. 1984. Adoptive transfer of myelin basic protein-sensitized T cells produces chronic relapsing demyelinating disease in mice. *Nature* 309: 356.

33 Wucherpfennig, K. W., Sette, A., Southwood, S. et al. 1994. Structural requirements for binding of an immunodominant myelin basic protein peptide to DR2 isotypes and for its recognition by human T cell clones. *J. Exp. Med.* 179: 279.

34 Tejada-Simon, M. V., Zang, Y. C., Yang, D. et al. 2000. Aberrant T cell responses to myelin antigens during clinical exacerbation in patients with multiple sclerosis. *Int. Immunol.* 12: 1,641.

35 Matsuzaki, G. and Umemura, M. 2007. Interleukin-17 as an effector molecule of innate and acquired immunity against infections. *Microbiol. Immunol.* 51: 1,139.

36 Wolk, K., Kunz, S., Witte, E., Friedrich, M., Asadullah, K. and Sabat, R. 2004. IL-22 increases the innate immunity of tissues. *Immunity* 21: 241.

37 Andoh, A., Zhang, Z., Inatomi, O. et al. 2005. Interleukin-22, a member of the IL-10 subfamily, induces inflammatory responses in colonic subepithelial myofibroblasts. *Gastroenterology* 129: 969.

38 Ikeuchi, H., Kuroiwa, T., Hiramatsu, N. et al. 2005. Expression of interleukin-22 in rheumatoid arthritis: potential role as a proinflammatory cytokine. *Arthritis Rheum.* 52: 1,037.

39 Langrish, C. L., Chen, Y., Blumenschein, W. M. et al. 2005. IL-23 drives a pathogenic T cell population that induces autoimmune inflammation. *J. Exp. Med.* 201: 233.

40 Radaeva, S., Sun, R., Pan, H. N., Hong, F. and Gao, B. 2004. Interleukin 22 (IL-22) plays a protective role in T cell-mediated murine hepatitis: IL-22 is a survival factor for hepatocytes via STAT3 activation. *Hepatology* 39: 1,332.

41 Zheng, Y., Danilenko, D. M., Valdez, P. et al. 2007. Interleukin-22, a T(H)17 cytokine, mediates IL-23-induced dermal inflammation and acanthosis. *Nature* 445: 648.

42 Kebir, H., Kreymborg, K., Ifergan, I. et al. 2007. Human TH17 lymphocytes promote blood-brain barrier disruption and central nervous system inflammation. *Nat. Med.* 13: 1,173.

43 Chang, H., Hanawa, H., Liu, H. et al. 2006. Hydrodynamic-based delivery of an interleukin-22-Ig fusion gene ameliorates experimental autoimmune myocarditis in rats. *J. Immunol.* 177: 3,635.

44 Zenewicz, L. A., Yancopoulos, G. D., Valenzuela, D. M., Murphy, A. J., Karow, M. and Flavell, R. A. 2007. Interleukin-22 but not interleukin-17 provides protection to hepatocytes during acute liver inflammation. *Immunity* 27: 647.

45 Kuchroo, V. K., Greer, J. M., Kaul, D. et al. 1994. A single TCR antagonist peptide inhibits experimental allergic encephalomyelitis mediated by a diverse T cell repertoire. *J. Immunol.* 153: 3,326.

46 Kuchroo, V. K., Sobel, R. A., Laning, J. C. et al. 1992. Experimental allergic encephalomyelitis mediated by cloned T cells specific for a synthetic peptide of myelin proteolipid protein. Fine specificity and T cell receptor V beta usage. *J. Immunol.* 148: 3,776.

47 Han, K. L., Lee, J., Kim, D. S., Park, S. J., Im, K. I. and Yong, T. S. 2006. Identification of differentially expressed cDNAs in *Acanthamoeba* culbertsoni after mouse brain passage. *Korean J. Parasitol.* 44: 15.

48 Marciano-Cabral, F. and Cabral, G. 2003. *Acanthamoeba* spp. as agents of disease in humans. *Clin. Microbiol. Rev.* 16: 273.